Mutations in *RAB39B* Cause X-Linked Intellectual Disability and Early-Onset Parkinson Disease with α-Synuclein Pathology

Gabrielle R. Wilson,[1,2] Joe C.H. Sim,[1] Catriona McLean,[3,4] Maila Giannandrea,[5,6] Charles A. Galea,[7] Jessica R. Riseley,[1] Sarah E.M. Stephenson,[1,2] Elizabeth Fitzpatrick,[1] Stefan A. Haas,[8] Kate Pope,[1] Kirk J. Hogan,[9] Ronald G. Gregg,[10] Catherine J. Bromhead,[11] David S. Wargowski,[12] Christopher H. Lawrence,[13] Paul A. James,[14] Andrew Churchyard,[15] Yujing Gao,[1] Dean G. Phelan,[1,2] Greta Gillies,[1] Nicholas Salce,[1] Lynn Stanford,[16] Ashley P.L. Marsh,[1,2] Maria L. Mignogna,[5,6] Susan J. Hayflick,[16] Richard J. Leventer,[1,2,17,18] Martin B. Delatycki,[1,2,19] George D. Mellick,[20] Vera M. Kalscheuer,[21] Patrizia D'Adamo,[5] Melanie Bahlo,[11,22,23] David J. Amor,[1,2] and Paul J. Lockhart[1,2,*]

Advances in understanding the etiology of Parkinson disease have been driven by the identification of causative mutations in families. Genetic analysis of an Australian family with three males displaying clinical features of early-onset parkinsonism and intellectual disability identified a ~45 kb deletion resulting in the complete loss of *RAB39B*. We subsequently identified a missense mutation (c.503C>A [p.Thr168Lys]) in *RAB39B* in an unrelated Wisconsin kindred affected by a similar clinical phenotype. In silico and in vitro studies demonstrated that the mutation destabilized the protein, consistent with loss of function. In vitro small-hairpin-RNA-mediated knockdown of *Rab39b* resulted in a reduction in the density of α-synuclein immunoreactive puncta in dendritic processes of cultured neurons. In addition, in multiple cell models, we demonstrated that knockdown of *Rab39b* was associated with reduced steady-state levels of α-synuclein. Post mortem studies demonstrated that loss of RAB39B resulted in pathologically confirmed Parkinson disease. There was extensive dopaminergic neuron loss in the substantia nigra and widespread classic Lewy body pathology. Additional pathological features included cortical Lewy bodies, brain iron accumulation, tau immunoreactivity, and axonal spheroids. Overall, we have shown that loss-of-function mutations in *RAB39B* cause intellectual disability and pathologically confirmed early-onset Parkinson disease. The loss of RAB39B results in dysregulation of α-synuclein homeostasis and a spectrum of neuropathological features that implicate RAB39B in the pathogenesis of Parkinson disease and potentially other neurodegenerative disorders.

Parkinsonism is a neurological syndrome characterized by tremor, rigidity, balance problems, and a slowing of movement. The most common cause of parkinsonism is Parkinson disease (PD [MIM 168600]), which accounts for up to 70% of this syndrome. PD is a common progressive neurodegenerative disorder with motor symptoms due to the death of dopamine-generating cells, predominantly in the substantia nigra (SN). The pathological hallmark of PD is accumulation of α-synuclein in Lewy bodies and Lewy neurites, although additional pathology (such as neurofibrillary tangles [NFTs]) can be observed.[1] Recent genetic studies have driven advances in understanding the molecular pathogenesis of PD, and preclinical discovery projects have investigated compounds that target the identified proteins as a precursor to etiology-based therapeutics. To date, 18 PD-associated loci have been reported, and variants in 13 monogenic or susceptibility genes have been identified.[2] Common pathogenic mechanisms associated with these genes include protein turnover, mitochondrial function, and oxidative-stress pathways. However, approximately 90% of individuals with PD do not have a defined genetic etiology. Variants in known genes account for ~10% of the variation in PD liability, suggesting that variants in additional genes and susceptibility loci remain to be identified.[3,4]

[1]Bruce Lefroy Centre for Genetic Health Research, Murdoch Childrens Research Institute, Melbourne, VIC 3052, Australia; [2]Department of Paediatrics, University of Melbourne, Melbourne, VIC 3052, Australia; [3]Anatomical Pathology, The Alfred, Melbourne, VIC 3181, Australia; [4]Australian Brain Bank Network, National Neuroscience Facility, Melbourne, VIC 3053, Australia; [5]Dulbecco Telethon Institute at Division of Neuroscience, San Raffaele Scientific Institute, Milan 20132, Italy; [6]Pharmaceutical Research and Early Development, Neuroscience, Ophthalmology, and Rare Diseases, F. Hoffmann-La Roche, Grenzacherstrasse 124, Basel 4070, Switzerland; [7]Medicinal Chemistry, Monash Institute of Pharmaceutical Sciences, Monash University, Melbourne, VIC 3052, Australia; [8]Department of Computational Molecular Biology, Max Planck Institute for Molecular Genetics, Ihnestrasse 73, Berlin 14195, Germany; [9]Department of Anesthesiology, School of Medicine and Public Health, University of Wisconsin, Madison, WI 53792, USA; [10]Department of Biochemistry and Molecular Biology, Center for Genetics and Molecular Medicine, University of Louisville, Louisville, KY 40202, USA; [11]Bioinformatics Division, Walter and Eliza Hall Institute, Melbourne, VIC 3052, Australia; [12]Waisman Center, Department of Pediatrics, University of Wisconsin School of Medicine and Public Health, Madison, WI 53705, USA; [13]Office of the State Forensic Pathologist, Royal Hobart Hospital, Hobart, TAS 7000, Australia; [14]Genetic Medicine Department, Royal Melbourne Hospital, Melbourne, VIC 3050, Australia; [15]Department of Neurology, Monash Children's Hospital, Melbourne, VIC 3168, Australia; [16]Department of Molecular and Medical Genetics, Oregon Health & Science University, Portland, OR 97239-3098, USA; [17]Murdoch Childrens Research Institute, Royal Children's Hospital, Melbourne, VIC 3052, Australia; [18]Department of Neurology, Royal Children's Hospital, Melbourne, VIC 3052, Australia; [19]Clinical Genetics, Austin Health, Melbourne, VIC 3084, Australia; [20]Eskitis Institute for Drug Discovery, Griffith University, Nathan, QLD 4111, Australia; [21]Department of Human Molecular Genetics, Max Planck Institute for Molecular Genetics, Ihnestrasse 73, Berlin 14195, Germany; [22]Department of Mathematics and Statistics, University of Melbourne, Melbourne, VIC 3010, Australia; [23]Department of Medical Biology, University of Melbourne, Melbourne, VIC 3010, Australia
*Correspondence: paul.lockhart@mcri.edu.au
http://dx.doi.org/10.1016/j.ajhg.2014.10.015.

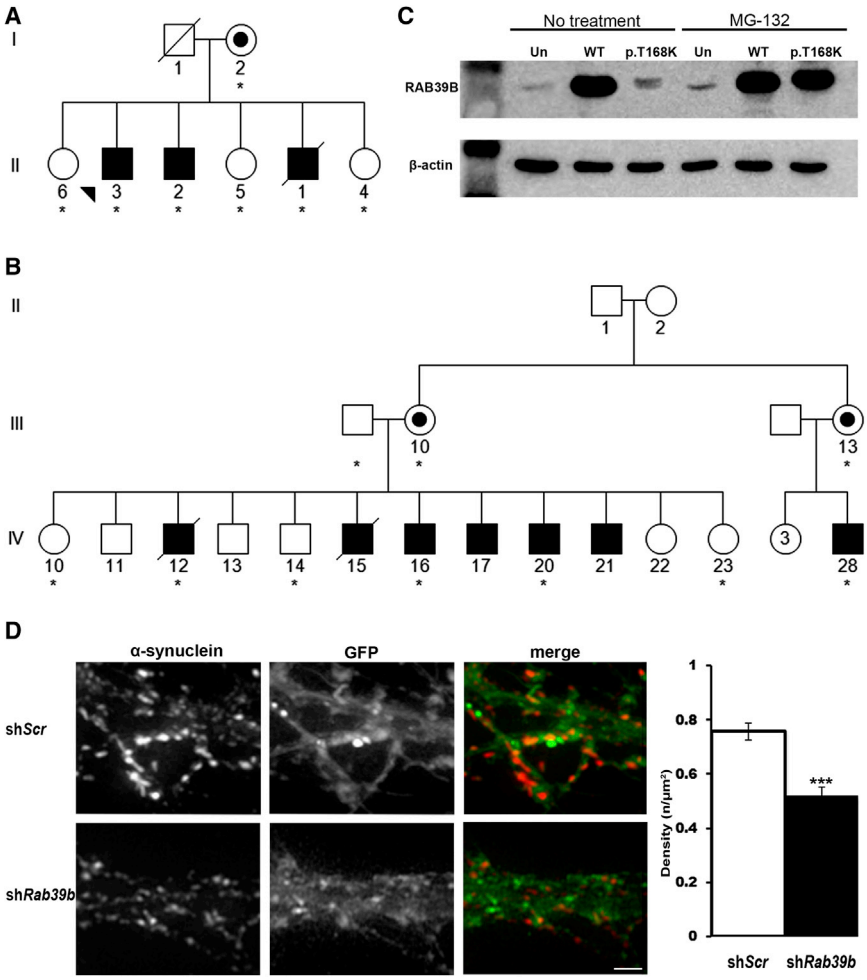

Figure 1. Identification of Mutations in *RAB39B*

(A and B) Simplified pedigree structure of the Australian (A) and Wisconsin (B) kindreds. Asterisks indicate DNA samples analyzed.

(C) Immunoblot analysis (12162-1-AP, Proteintech; 1:1,000) of RAB39B in BE(2)-M17 neuroblastoma cells grown in the absence or presence of 10 μM MG-132. Abbreviations are as follows: Un, untransfected; WT, wild-type; and p.T168K, RAB39B p.Thr168Lys. β-actin was used for confirming equivalent protein loading (A5441, Sigma-Aldrich; 1:5,000).

(D) Representative images of mouse hippocampal neurons transduced with lentiviral vectors encoding GFP and either scramble (sh*Scr*) or sh*Rab39b* sequences. Images were captured, and Z-space slices (0.3–0.4 μm) were deconvolved and flattened by maximum projection. ImageJ analysis software (the "Gran filter" plug-in set the size from 1 to infinity) was used to measure α-synuclein density relative to the area of infected dendrites. Quantification showed a significant reduction (0.52 ± 0.03 versus 0.76 ± 0.03, mean ± SEM, $p \leq 0.0005$) in the density of α-synuclein immunoreactive puncta in neurons downregulated for *Rab39b*. The experiment was performed in triplicate (n = 42 neurons scored). The scale bar represents 20 μm.

We identified an Australian kindred with three brothers who presented in childhood with nonprogressive intellectual disability (ID), which included delayed developmental milestones, cognitive impairment, and macrocephaly (Figure 1; Table S1, available online). Subsequently, early-onset parkinsonism (onset prior to 45 years of age) was also apparent, although the clinical progression and presentation varied. The proband developed tremor in late childhood, but the symptoms did not progress to frank parkinsonism. In contrast, his male siblings developed tremor from their late 30s and were diagnosed with L-DOPA-responsive akinetic-rigid PD by their mid-40s. A complete description of the phenotype is presented in Table S1. We collected samples from the Australian family after receiving institutional ethics approval from Royal Childrens Hospital (Melbourne) and written informed consent from participants. Genomic DNA was isolated from whole blood, and primary fibroblast cultures were generated according to standard protocols. SNP array and linkage analysis using a recessive homozygous model did not demonstrate linkage to the autosomes but did identify two ~10.6 Mb haplotypes shared by the affected brothers at Xp22.2 and Xq27.3–qter (chrX: 3,624,034–14,291,092 and chrX: 145,644,895–tel, respectively; GRCh38/hg38, UCSC Genome Browser; Table S2). Copy-number variation and subsequent PCR analysis identified a ~45 kb deletion within the Xq haplotype (ClinVar accession number SCV00019029). The deletion segregated with the disease and resulted in the complete deletion of *RAB39B* (RAB39B, member RAS oncogene family [MIM 300774]) and the last three coding exons of *CLIC2* (chloride intracellular channel 2 [MIM 300138]). To assess *RAB39B* expression, we extracted total RNA from fibroblasts by using the SV Total RNA Isolation System (Promega) and synthesized cDNA with the Transcriptor First Strand cDNA Synthesis Kit (Roche). Consistent with the genomic data, the *RAB39B* and *CLIC2* transcripts were not detected by RT-PCR analysis of fibroblast cells derived from affected individuals (Figure S1).

The phenotype of the Australian kindred is similar to the basal ganglia disorder (Waisman syndrome [MIM 311510]) reported for a Wisconsin kindred[5] (Figure 1; Table S1). Members of the defining family included 13 affected males who presented with variable degrees of ID and early-onset parkinsonism. Multipoint linkage analysis of the Wisconsin family previously localized the disease-causing mutation to Xq27.3–qter with a maximum multipoint LOD of 6.75 at the genetic marker F8C (chrX:154,929,351–154,929,630; GRCh38/hg38). The minimal Xq linkage region in the Australian kindred is within the Xq27.3–qter interval and therefore defines the shared critical linkage interval.[6]

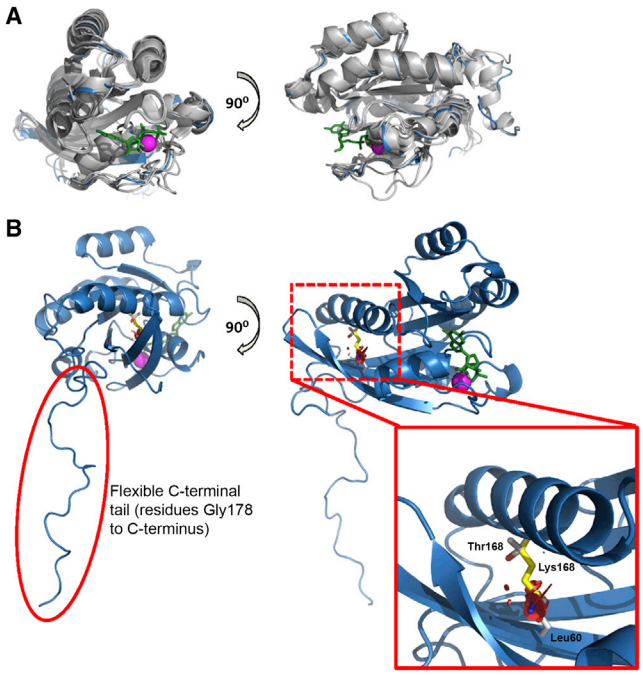

Figure 2. In Silico Modeling of the RAB39B Structure Predicts that p.Thr168Lys Is Destabilizing

(A) We generated a molecular model of the RAB39B structure (blue) by superimposing the structures of several known RAB proteins (gray) available in the Protein Data Bank (YTP1 [PDB 2BCG], RAB1A [PDB 3TKL], RAB11B [PDB 2F9L], RAB18 [PDB 1X3S], RAB23 [PDB 1Z2A], and RAB30 [PDB 2EW1]). GTP (green sticks) and Mg^{2+} (magenta sphere) are from the structure of RAB5A after superposition.

(B) We then used the predicted RAB39B structure (blue) to model the position of the native (Thr168, red) and altered (Lys168, yellow) amino acid. In the native form, Thr168 is predicted to interact with Leu60 within the interswitch region of RAB39B. The internal placement of the large positively charged residue in the p.Thr168Lys protein is predicted to destabilize the protein. The quality of the model was tested with PROCHECK,[12] ANOLEA,[13] and Verify3D.[14]

Genomic DNA from individuals of the Wisconsin kindred was kindly provided by Professor Ronald Gregg. Ethics approval was provided by the institutional review board (IRB) at the University of Wisconsin, and informed consent was obtained. Direct sequencing of *RAB39B* identified a missense mutation (c.503C>A [p.Thr168Lys]; RefSeq accession number NM_171998.2, ClinVar SCV000190018) that segregated with disease (Figure S2) and was not detected in 200 unrelated control individuals or public databases (dbSNP137 and ESP6500). The threonine residue is conserved in evolution (Figure S3), and the mutation is predicted to be damaging by PolyPhen-2 and SIFT. In contrast, no sequence variants were observed by direct sequencing of *CLIC2* in the Wisconsin kindred.

The absence of mutations in *CLIC2* in the Wisconsin kindred suggests that disruption of *RAB39B* is the cause of the shared phenotype in both families. It is possible that deletion of *CLIC2* in the Australian kindred might act as a disease modifier, although the phenotypic features (seizures and cardiac anomalies) associated with a missense mutation in *CLIC2* were not observed.[7] X chromosome exome sequencing of affected males from both kindreds confirmed the deleterious *RAB39B* changes and did not identify any other candidate variants within the linkage regions (Table S3).

In silico modeling of RAB39B was performed with the structure prediction programs MODELER[8] and HHpred,[9] and protein structures were visualized and superimposed with PyMOL. This analysis suggested that Thr168 is buried within the wild-type protein and interacts with Leu60 in the interswitch region, which undergoes conformational changes upon GTP-GDP exchange[10,11] (Figure 2). The mutation introduces a large, positively charged lysine residue that is predicted by multiple algorithms, including ERIS[15] and PoPMuSiC,[16] to destabilize the protein. We could not directly test this because endogenous RAB39B was not detectable in fibroblast cells; therefore, we generated stable BE(2)-M17 neuroblastoma lines overexpressing wild-type RAB39B and altered (p.Thr168 Lys) RAB39B. The complete *RAB39B* open reading frame was amplified from human brain cDNA and cloned into the mammalian expression vector pcDNA3.1 (Invitrogen). We used site-directed mutagenesis (QuickChangeII) to generate the p.Thr168Lys altered RAB39B construct and Sanger sequenced all clones to verify that no additional variants were present. RT-PCR analysis confirmed similar expression of the wild-type and altered constructs (data not shown). In contrast, immunoblot analysis revealed high steady-state levels of exogenous wild-type RAB39B but very low levels of exogenous altered RAB39B. Immunoblot and immunofluorescence analysis of the cells after treatment with the proteasome inhibitor MG-132 confirmed that the reduced steady-state level of altered RAB39B was due to rapid turnover of the protein by the ubiquitin proteasome system (Figure 1; Figure S4). These results confirm the in silico modeling suggesting that the altered protein is destabilized and collectively demonstrate that loss of function of RAB39B causes ID and parkinsonism. Previous studies have associated *RAB39B* mutations with ID[17–19] (pedigrees D-23 and MRX72; Table S1). The absence of parkinsonism in these additional families could be due to the individuals' age at reporting, given that our data suggest that parkinsonism is likely to manifest after the second decade, albeit with some variability in both onset and clinical severity (Table S1). However, the lack of clinical data and inability to re-examine affected individuals mean that it is difficult to determine whether the phenotype associated with loss of RAB39B function represents an age-dependent progression of ID and parkinsonism or a spectrum of heterogeneous phenotypes extending from ID to ID with parkinsonism (see below).

Rab GTPases belong to the Ras superfamily of small GTPases and act as essential regulators of vesicular trafficking. They dynamically localize to distinct intracellular membranes and regulate vesicular transport by recruiting effector proteins.[20] The precise localization and function of RAB39B is unknown, but the protein is thought to play a role in synapse formation and maintenance.[17,18,21]

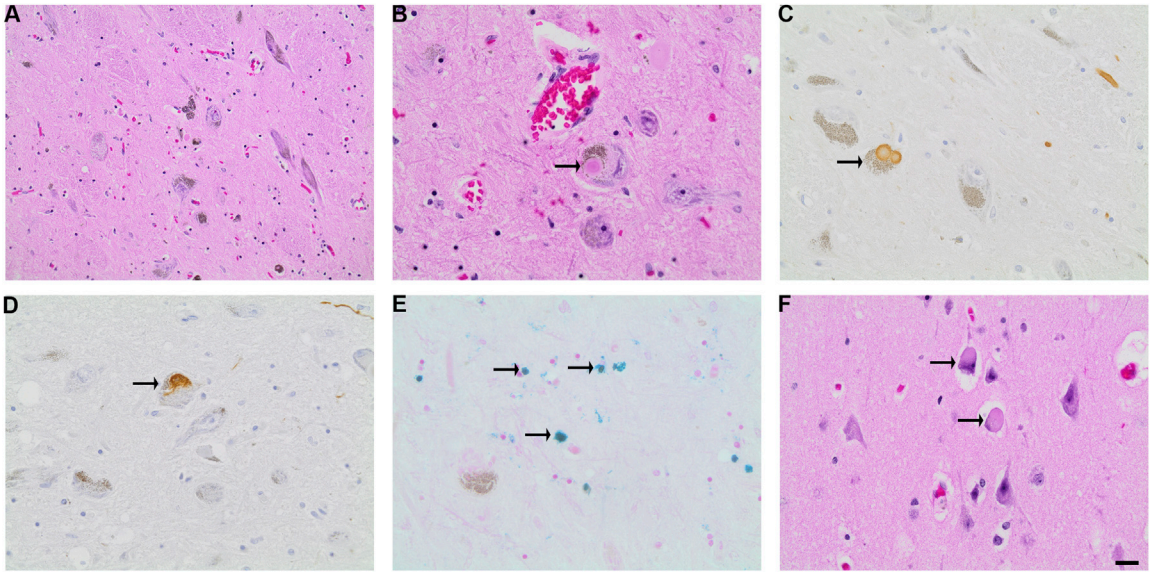

Figure 3. Neuropathology Associated with Loss of RAB39B
CNS postmortem tissue from II:1 was collected at autopsy, and microscopic examination was performed on H&E-stained sections. To detect PD-associated proteins, we applied immunohistochemistry to 5 μm formalin-fixed paraffin-embedded sections as previously described.[25] Primary antibodies utilized were anti-α-synuclein (97/8; 1:1,000)[23] and anti-tau (A0024, Dako; 1:500). CNS nonhaem iron (Fe^{2+} and Fe^{3+}) was detected with a previously described Perl's methodology.[26] The scale bar represents 50 μm (A) or 20 μm (B–F). (A–E) SN sections show (A) neuronal loss and pigment incontinence (H&E), (B) intraneuronal Lewy bodies (H&E), (C) α-synuclein-reactive Lewy bodies and neurites, (D) tau-immunoreactive intraneuronal NFTs, and (E) extracellular iron deposition (Perl's stain). (F) Neocortical Lewy bodies were identified by H&E staining.

In support of this, we observed colocalization of endogenous RAB39B with markers of the vesicular-transport pathway, particularly the early endosome in mouse and human neuroblastoma cells (Figure S5). Given the postmortem results (below) and the association between α-synuclein and vesicular-trafficking pathways,[22] we tested the effect of downregulation of RAB39B on α-synuclein localization. Mouse hippocampal neurons were prepared and transduced with lentivirus expressing validated *Rab39b* small hairpin RNA (shRNA) as previously described.[17] Fourteen days after transduction, we observed that the density of α-synuclein immunoreactive puncta in the dendritic processes was 30% lower than in the cells transduced with the scramble control shRNA ($p \leq 0.0005$; Figure 1; Figure S6). Immunoblot analysis confirmed ~40% reduction of RAB39B but also demonstrated that α-synuclein levels (detected with the anti-α-synuclein antibody 97/8,[23] 1:1,000) were reduced by ~50% ($p \leq 0.05$; Figure S6). Similarly, in P19 mouse neuroblastoma cells, immunoblot analysis demonstrated that shRNA-mediated knockdown of *Rab39b* resulted in ~50% reduction in α-synuclein steady-state levels ($p \leq 0.005$; Figure S6). Although the mechanism remains to be fully defined, these results suggest that downregulation of RAB39B results in dysregulation of α-synuclein homeostasis. We sequenced *RAB39B* in a cohort of 187 individuals with early-onset PD; they had been previously sequenced and shown not to have mutations in known PD-associated genes, including *SNCA* (MIM 163890), *PARK2* (MIM 602544), *DJ1* (MIM 602533), *PINK1* (MIM 608309), and *LRRK2* (MIM 609007).[24] This analysis did not identify any additional variants, suggesting that mutations in *RAB39B* are not a common cause of early-onset PD.

To determine whether the parkinsonism observed in the affected individuals resulted from PD, we investigated the neuropathology associated with the loss of *RAB39B*. Individual II:1 died at age 48 years from positional asphyxia. Postmortem neuropathological studies on the brain of II:1 were consistent with PD. The macroscopic findings were unremarkable, and serial coronal sections showed normal cortex, white matter, and ventricles with normal-appearing basal ganglia and thalamus. Cross section of the brain stem showed pallor of the SN and locus coeruleus. SN sections stained with haematoxylin and eosin (H&E) revealed hallmark neuropathological PD features, including loss of pigmented neurons and Lewy bodies in surviving neurons (Figure 3). Immunoreactive staining revealed the presence of α-synuclein-positive Lewy bodies and Lewy neurites in >10% of the surviving neurons. Additional neuropathological features included an abundance of cortical Lewy bodies, which are a pathological feature characteristic of dementia with Lewy bodies (DLB [MIM 127750]; reviewed in[27,28]). Tau-immunoreactive NFTs were also observed in a small proportion of the surviving pigmented SN neurons (Figure 3). Tau pathology has previously been observed in familial and idiopathic PD, and the tau-encoding gene (microtubule-associated protein tau [*MAPT* (MIM 157140)]) exists within a PD susceptibility locus. Tau plays a role in iron homeostasis,[29–31] and Perl staining revealing a modest accumulation of iron in the

SN (Figure 3) was consistent with the slight reduction in T2 signal intensity observed in individual II:1 (Table S1). In addition, analysis of the basal ganglia identified rare axonal spheroids in the white-matter tracts (data not shown), similar to the Wallerian-like degeneration observed in neurodegenerative diseases with impaired axonal transport.[32] The additional pathological and clinical features share similarities with other neurodegenerative disorders, the most similar of which was neurodegeneration with brain iron accumulation (NBIA [MIM 234200]). Notably, in rare cases, NBIA can manifest with developmental delay and subsequent early-onset parkinsonism.[33] Although MRI of II:3 was normal and II:1 did not show symptoms typical of NBIA,[34] genomic DNA from individuals with NBIA was analyzed. Ethics approval was provided by the IRB at Oregon Health & Science University, and informed consent was obtained. Sequence analysis of *RAB39B* in a cohort of 48 male individuals with NBIA of unknown etiology did not identify any variants.

In conclusion, genetic studies have demonstrated that loss of RAB39B causes pathologically defined PD, and functional studies have provided additional evidence for pathogenicity. Our results link the loss of a single gene involved in neuronal organization and synaptic function to the early manifestation of both ID and neurodegeneration and suggest that the loss of RAB39B dysregulates α-synuclein. For the two families we ascertained and clinically characterized, there appears to be a canonical age-dependent progression, namely ID first and then a slowly progressive basal ganglia disorder that advances after puberty. This was observed or reported in all 16 affected males in the Australian and Wisconsin families. However, given the lack of clinical data for the other two families previously described to be affected by *RAB39B* mutations,[17] it is unclear whether this age-dependent phenotype predominates or whether heterogeneous phenotypes extending from ID to ID with parkinsonism are associated with loss of RAB39B function. This issue will be resolved by future studies of additional individuals with mutations in *RAB39B*.

The proposed role of RAB39B in vesicular trafficking identifies a potential disease mechanism that is distinct from pathways associated with genes in which mutations are currently known to cause familial early-onset PD. Previous in vitro studies have demonstrated that α-synuclein-mediated deficits in vesicular trafficking can be ameliorated by the overexpression of several RAB proteins[35,36] but have not shown that loss of a specific RAB can cause PD. Current studies are further investigating how loss of RAB39B might cause the observed in vitro deficits in localization and reduced steady-state levels of α-synuclein but in vivo accumulation of significant α-synuclein pathology at end-stage disease. It is possible that in simple cell models with efficient protein-metabolism pathways, the "mislocalized" α-synuclein is rapidly turned over and thus leads to reduced steady-state levels. However, protein-turnover pathways are compromised in individuals with PD;[37] therefore, mislocalized α-synuclein might not be turned over efficiently, and as the disease progresses, the protein could accumulate and be incorporated into the protein aggregates that define PD.

The broader pathology of iron accumulation, NFTs, and axonal spheroids is similar to that reported for a range of neurodegenerative conditions. However, the abundance of both brainstem and cortical Lewy bodies suggests that RAB39B and/or associated pathways might directly contribute to the pathogenic mechanisms underlying dementia disorders such as DLB. Further studies, including the development of animal models, will be important for understanding the underlying pathogenic mechanism(s) of RAB39B dysfunction and identifying potential targeted therapeutic interventions.

Supplemental Data

Supplemental Data include six figures and three tables and can be found with this article online at http://dx.doi.org/10.1016/j.ajhg.2014.10.015.

Acknowledgments

We thank the families for their participation in this study and the generous support of the Lefroy and Handbury families. This work was funded in part by Australian National Health and Medical Research Council (NHMRC) program grant 490037 to D.J.A. and M.B., NHMRC project grant APP1041860 to P.J.L., Parkinson's Disease Foundation grant PDF-IRG-1220 to P.J.L. and G.R.W., and the project GENCODYS (grant 241995 to V.M.K.), which was funded by the European Union Framework Programme 7. P.J.L. was supported by an NHMRC Career Development Fellowship (APP1032364), and M.B. was supported by an Australian Research Council Future Fellowship (FT100100764). This work was made possible through Victorian State Government Operational Infrastructure Support and the NHMRC Independent Medical Research Institutes Infrastructure Support Scheme.

Received: September 22, 2014
Accepted: October 30, 2014
Published: November 26, 2014

Web Resources

The URLs for data presented herein are as follows:

ClinVar, http://www.ncbi.nlm.nih.gov/clinvar/
Online Mendelian Inheritance in Man (OMIM), http://www.omim.org/
PyMOL, http://www.pymol.org/
RefSeq, http://www.ncbi.nlm.nih.gov/refseq/

Accession Numbers

The ClinVar accession numbers for the *RAB39B* variants reported in this paper are SCV000190018 and SCV000190929.

References

1. Galpern, W.R., and Lang, A.E. (2006). Interface between tauopathies and synucleinopathies: a tale of two proteins. Ann. Neurol. *59*, 449–458.

2. Klein, C., and Westenberger, A. (2012). Genetics of Parkinson's disease. Cold Spring Harb. Perspect. Med. *2*, a008888.
3. Do, C.B., Tung, J.Y., Dorfman, E., Kiefer, A.K., Drabant, E.M., Francke, U., Mountain, J.L., Goldman, S.M., Tanner, C.M., Langston, J.W., et al. (2011). Web-based genome-wide association study identifies two novel loci and a substantial genetic component for Parkinson's disease. PLoS Genet. *7*, e1002141.
4. Keller, M.F., Saad, M., Bras, J., Bettella, F., Nicolaou, N., Simón-Sánchez, J., Mittag, F., Büchel, F., Sharma, M., Gibbs, J.R., et al.; International Parkinson's Disease Genomics Consortium (IPDGC); Wellcome Trust Case Control Consortium 2 (WTCCC2) (2012). Using genome-wide complex trait analysis to quantify 'missing heritability' in Parkinson's disease. Hum. Mol. Genet. *21*, 4996–5009.
5. Laxova, R., Brown, E.S., Hogan, K., Hecox, K., and Opitz, J.M. (1985). An X-linked recessive basal ganglia disorder with mental retardation. Am. J. Med. Genet. *21*, 681–689.
6. Gregg, R.G., Metzenberg, A.B., Hogan, K., Sekhon, G., and Laxova, R. (1991). Waisman syndrome, a human X-linked recessive basal ganglia disorder with mental retardation: localization to Xq27.3-qter. Genomics *9*, 701–706.
7. Takano, K., Liu, D., Tarpey, P., Gallant, E., Lam, A., Witham, S., Alexov, E., Chaubey, A., Stevenson, R.E., Schwartz, C.E., et al. (2012). An X-linked channelopathy with cardiomegaly due to a CLIC2 mutation enhancing ryanodine receptor channel activity. Hum. Mol. Genet. *21*, 4497–4507.
8. Eswar, N., Webb, B., Marti-Renom, M.A., Madhusudhan, M.S., Eramian, D., Shen, M.Y., Pieper, U., and Sali, A. (2006). Comparative protein structure modeling using Modeller. Curr. Protoc. Bioinformatics *Chapter 5*, Unit 5.6.
9. Hildebrand, A., Remmert, M., Biegert, A., and Söding, J. (2009). Fast and accurate automatic structure prediction with HHpred. Proteins *77* (*Suppl 9*), 128–132.
10. Khan, A.R., and Ménétrey, J. (2013). Structural biology of Arf and Rab GTPases' effector recruitment and specificity. Structure *21*, 1284–1297.
11. Park, H.H. (2013). Structural basis of membrane trafficking by rab family small g protein. Int. J. Mol. Sci. *14*, 8912–8923.
12. Laskowski, R.A., Moss, D.S., and Thornton, J.M. (1993). Main-chain bond lengths and bond angles in protein structures. J. Mol. Biol. *231*, 1049–1067.
13. Melo, F., Devos, D., Depiereux, E., and Feytmans, E. (1997). ANOLEA: a www server to assess protein structures. Proc. Int. Conf. Intell. Syst. Mol. Biol. *5*, 187–190.
14. Eisenberg, D., Lüthy, R., and Bowie, J.U. (1997). VERIFY3D: assessment of protein models with three-dimensional profiles. Methods Enzymol. *277*, 396–404.
15. Yin, S., Ding, F., and Dokholyan, N.V. (2007). Eris: an automated estimator of protein stability. Nat. Methods *4*, 466–467.
16. Dehouck, Y., Kwasigroch, J.M., Gilis, D., and Rooman, M. (2011). PoPMuSiC 2.1: a web server for the estimation of protein stability changes upon mutation and sequence optimality. BMC Bioinformatics *12*, 151.
17. Giannandrea, M., Bianchi, V., Mignogna, M.L., Sirri, A., Carrabino, S., D'Elia, E., Vecellio, M., Russo, S., Cogliati, F., Larizza, L., et al. (2010). Mutations in the small GTPase gene RAB39B are responsible for X-linked mental retardation associated with autism, epilepsy, and macrocephaly. Am. J. Hum. Genet. *86*, 185–195.
18. Vanmarsenille, L., Giannandrea, M., Fieremans, N., Verbeeck, J., Belet, S., Raynaud, M., Vogels, A., Männik, K., Õunap, K., Jacqueline, V., et al. (2014). Increased dosage of RAB39B affects neuronal development and could explain the cognitive impairment in male patients with distal Xq28 copy number gains. Hum. Mutat. *35*, 377–383.
19. Russo, S., Cogliati, F., Cavalleri, F., Cassitto, M.G., Giglioli, R., Toniolo, D., Casari, G., and Larizza, L. (2000). Mapping to distal Xq28 of nonspecific X-linked mental retardation MRX72: linkage analysis and clinical findings in a three-generation Sardinian family. Am. J. Med. Genet. *94*, 376–382.
20. Hutagalung, A.H., and Novick, P.J. (2011). Role of Rab GTPases in membrane traffic and cell physiology. Physiol. Rev. *91*, 119–149.
21. Cheng, H., Ma, Y., Ni, X., Jiang, M., Guo, L., Ying, K., Xie, Y., and Mao, Y. (2002). Isolation and characterization of a human novel RAB (RAB39B) gene. Cytogenet. Genome Res. *97*, 72–75.
22. Eisbach, S.E., and Outeiro, T.F. (2013). Alpha-synuclein and intracellular trafficking: impact on the spreading of Parkinson's disease pathology. J. Mol. Med. *91*, 693–703.
23. Culvenor, J.G., McLean, C.A., Cutt, S., Campbell, B.C., Maher, F., Jäkälä, P., Hartmann, T., Beyreuther, K., Masters, C.L., and Li, Q.X. (1999). Non-Abeta component of Alzheimer's disease amyloid (NAC) revisited. NAC and alpha-synuclein are not associated with Abeta amyloid. Am. J. Pathol. *155*, 1173–1181.
24. Mellick, G.D., Siebert, G.A., Funayama, M., Buchanan, D.D., Li, Y., Imamichi, Y., Yoshino, H., Silburn, P.A., and Hattori, N. (2009). Screening PARK genes for mutations in early-onset Parkinson's disease patients from Queensland, Australia. Parkinsonism Relat. Disord. *15*, 105–109.
25. Fodero-Tavoletti, M.T., Smith, D.P., McLean, C.A., Adlard, P.A., Barnham, K.J., Foster, L.E., Leone, L., Perez, K., Cortés, M., Culvenor, J.G., et al. (2007). In vitro characterization of Pittsburgh compound-B binding to Lewy bodies. J. Neurosci. *27*, 10365–10371.
26. Meguro, R., Asano, Y., Odagiri, S., Li, C., and Shoumura, K. (2008). Cellular and subcellular localizations of nonheme ferric and ferrous iron in the rat brain: a light and electron microscopic study by the perfusion-Perls and -Turnbull methods. Arch. Histol. Cytol. *71*, 205–222.
27. Huang, Y., and Halliday, G. (2013). Can we clinically diagnose dementia with Lewy bodies yet? Transl. Neurodegener. *2*, 4.
28. Mrak, R.E., and Griffin, W.S. (2007). Dementia with Lewy bodies: Definition, diagnosis, and pathogenic relationship to Alzheimer's disease. Neuropsychiatr. Dis. Treat. *3*, 619–625.
29. Simón-Sánchez, J., Schulte, C., Bras, J.M., Sharma, M., Gibbs, J.R., Berg, D., Paisan-Ruiz, C., Lichtner, P., Scholz, S.W., Hernandez, D.G., et al. (2009). Genome-wide association study reveals genetic risk underlying Parkinson's disease. Nat. Genet. *41*, 1308–1312.
30. Lei, P., Ayton, S., Finkelstein, D.I., Spoerri, L., Ciccotosto, G.D., Wright, D.K., Wong, B.X., Adlard, P.A., Cherny, R.A., Lam, L.Q., et al. (2012). Tau deficiency induces parkinsonism with dementia by impairing APP-mediated iron export. Nat. Med. *18*, 291–295.
31. Wray, S., and Lewis, P.A. (2010). A tangled web - tau and sporadic Parkinson's disease. Front. Psychiatry *1*, 150.
32. Coleman, M.P., and Freeman, M.R. (2010). Wallerian degeneration, wld(s), and nmnat. Annu. Rev. Neurosci. *33*, 245–267.
33. Gregory, A., Polster, B.J., and Hayflick, S.J. (2009). Clinical and genetic delineation of neurodegeneration with brain iron accumulation. J. Med. Genet. *46*, 73–80.

34. Schipper, H.M. (2012). Neurodegeneration with brain iron accumulation - clinical syndromes and neuroimaging. Biochim. Biophys. Acta *1822*, 350–360.
35. Cooper, A.A., Gitler, A.D., Cashikar, A., Haynes, C.M., Hill, K.J., Bhullar, B., Liu, K., Xu, K., Strathearn, K.E., Liu, F., et al. (2006). Alpha-synuclein blocks ER-Golgi traffic and Rab1 rescues neuron loss in Parkinson's models. Science *313*, 324–328.
36. Gitler, A.D., Bevis, B.J., Shorter, J., Strathearn, K.E., Hamamichi, S., Su, L.J., Caldwell, K.A., Caldwell, G.A., Rochet, J.C., McCaffery, J.M., et al. (2008). The Parkinson's disease protein alpha-synuclein disrupts cellular Rab homeostasis. Proc. Natl. Acad. Sci. USA *105*, 145–150.
37. Cook, C., Stetler, C., and Petrucelli, L. (2012). Disruption of protein quality control in Parkinson's disease. Cold Spring Harb. Perspect. Med. *2*, a009423.

The American Journal of Human Genetics, Volume *95*

Supplemental Data

Mutations in *RAB39B* Cause X-Linked Intellectual Disability and Early-Onset Parkinson Disease with α-Synuclein Pathology

Gabrielle R. Wilson, Joe C.H. Sim, Catriona McLean, Maila Giannandrea, Charles A. Galea, Jessica R. Riseley, Sarah E.M. Stephenson, Elizabeth Fitzpatrick, Stefan A. Haas, Kate Pope, Kirk J. Hogan, Ronald G. Gregg, Catherine J. Bromhead, David S. Wargowski, Christopher H. Lawrence, Paul A. James, Andrew Churchyard, Yujing Gao, Dean G. Phelan, Greta Gillies, Nicholas Salce, Lynn Stanford, Ashley P.L. Marsh, Maria L. Mignogna, Susan J. Hayflick, Richard J. Leventer, Martin B. Delatycki, George D. Mellick, Vera M. Kalscheuer, Patrizia D'Adamo, Melanie Bahlo, David J. Amor, and Paul J. Lockhart

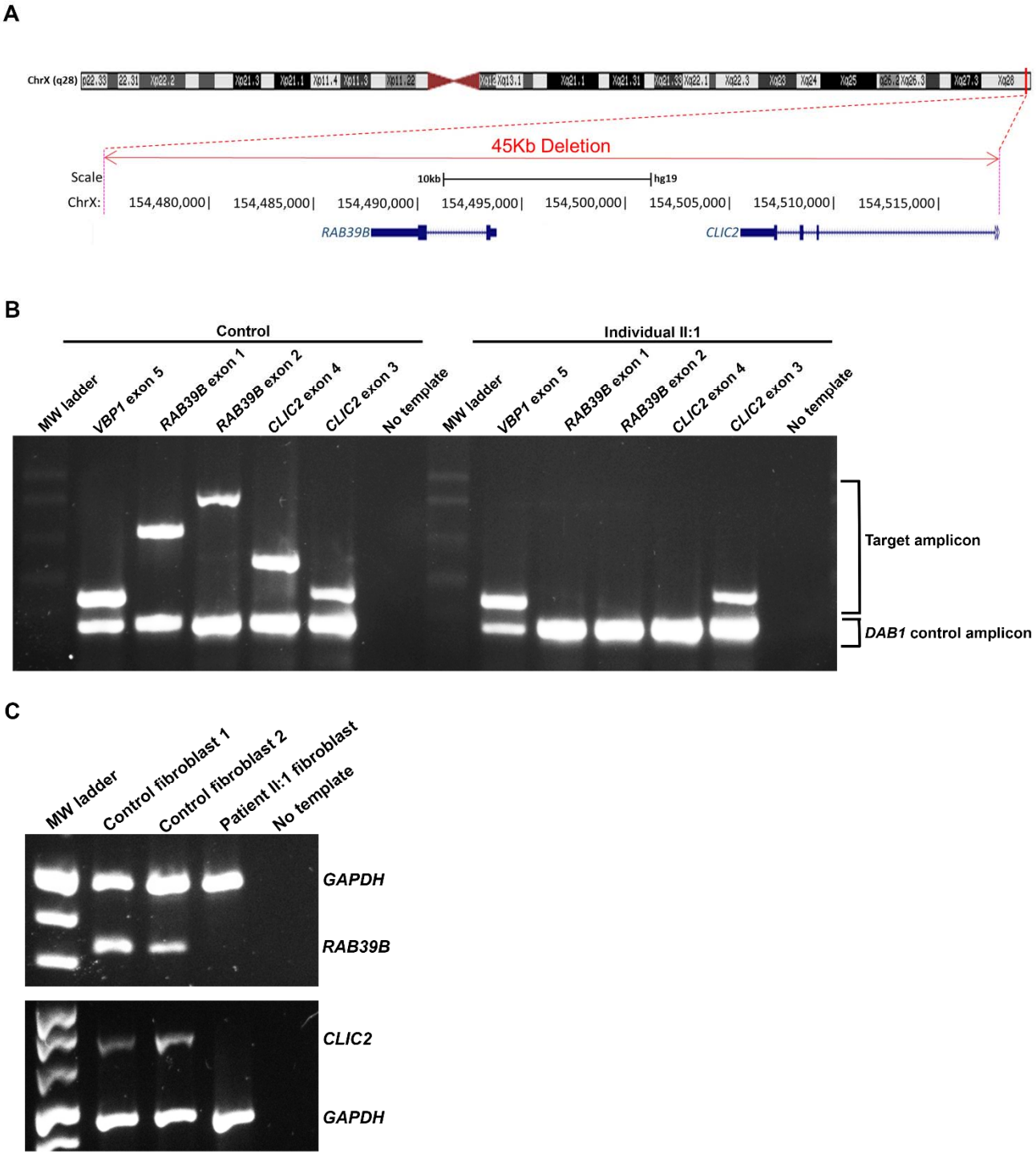

Figure S1: Confirmation of *RAB39B* deletion in the Australian pedigree.

(A) CNV analysis identified a 45Kb deletion spanning Hg19 ChrX: 154,474,499-154,518,072 that resulted in the deletion of *RAB39B* and the last three exons of *CLIC2*. (B) PCR amplification of *RAB39B* (NG_012626.2) and the surrounding genes, *VBP1* (MIM300133) and *CLIC2* was achieved using primer pairs available on request. A duplex PCR amplifying an independent control gene (*DAB1* [MIM603448]) was performed to confirm the deletion of *RAB39B* and *CLIC2* in the Australian kindred. (C) End-point RT-PCR analysis of fibroblast RNA confirmed the absence of *RAB39B* and *CLIC2* expression in individual II:1. The reactions were duplexed with a primer set targeting *GAPDH* (MIM138400) to confirm template integrity.

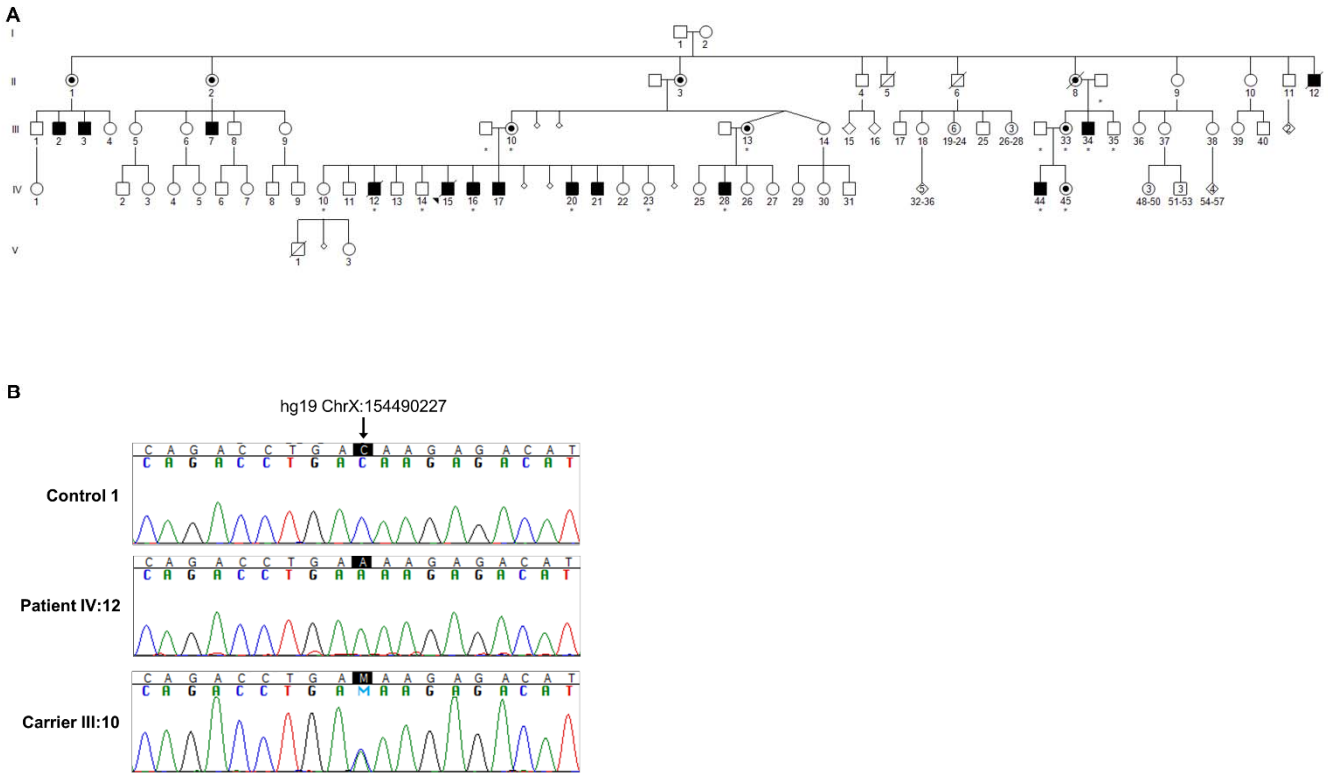

Figure S2: Confirmation of the NM_171998.2: c.503C>A (p.Thr168Lys) mutation in *RAB39B*

(A) Full pedigree of the previously published Wisconsin kindred. Affected males and obligate female carriers are represented by the filled squares and circles with dots respectively. (B) Representative sequence traces confirming the NM_171998.2: c.503C>A, p.Thr168Lys mutation. Sanger sequencing was performed using standard protocols, amplicons were sequenced using Big Dye Terminator v3.1 (Applied Biosystems) and Sequencher software (Gene Codes) was used to analyse sequence traces. * represent individuals with DNA collected.

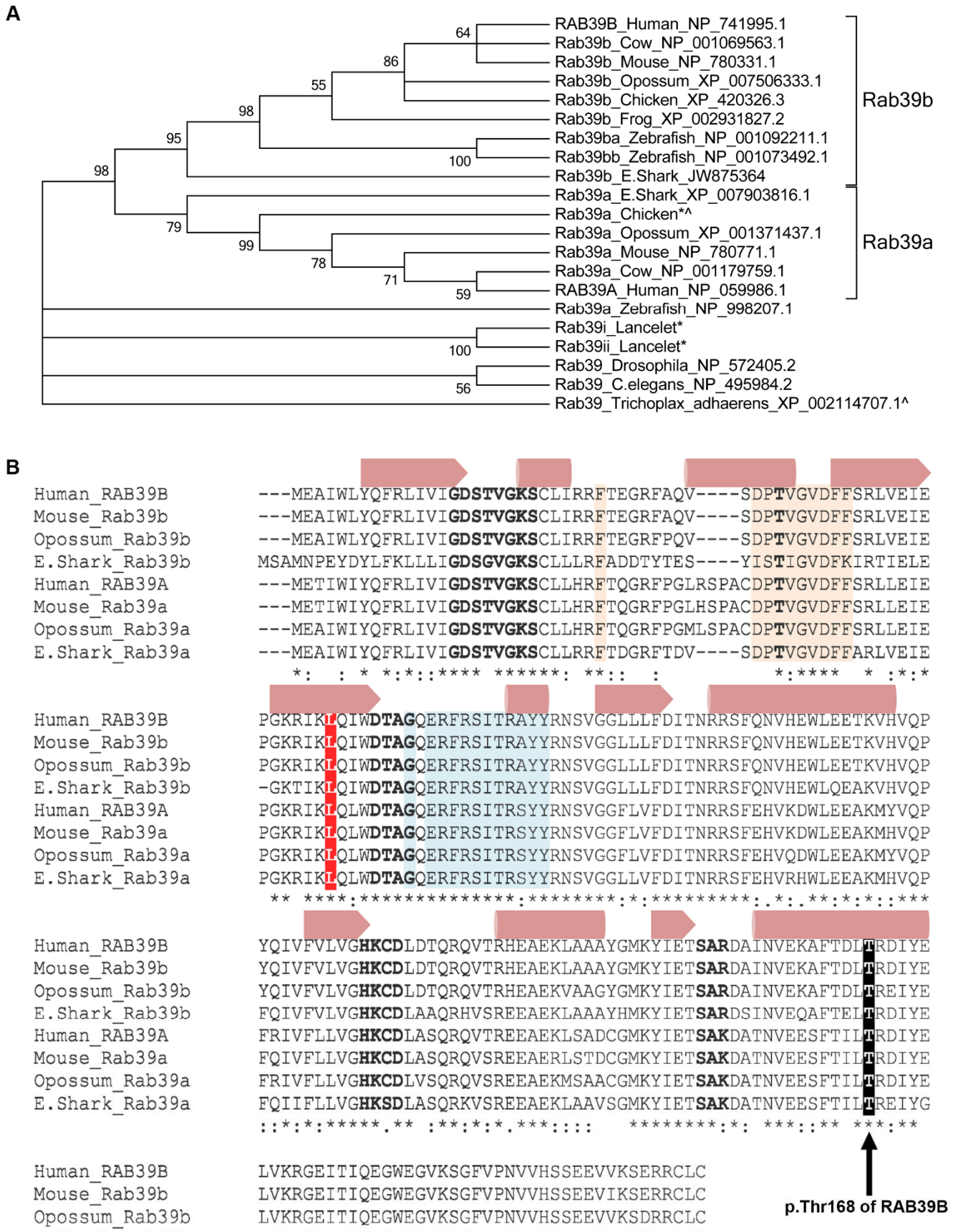
A
RAB39B_Human_NP_741995.1
Rab39b_Cow_NP_001069563.1
Rab39b_Mouse_NP_780331.1
Rab39b_Opossum_XP_007506333.1
Rab39b_Chicken_XP_420326.3
Rab39b_Frog_XP_002931827.2
Rab39ba_Zebrafish_NP_001092211.1
Rab39bb_Zebrafish_NP_001073492.1
Rab39b_E.Shark_JW875364
Rab39a_E.Shark_XP_007903816.1
Rab39a_Chicken*^
Rab39a_Opossum_XP_001371437.1
Rab39a_Mouse_NP_780771.1
Rab39a_Cow_NP_001179759.1
RAB39A_Human_NP_059986.1
Rab39a_Zebrafish_NP_998207.1
Rab39i_Lancelet*
Rab39ii_Lancelet*
Rab39_Drosophila_NP_572405.2
Rab39_C.elegans_NP_495984.2
Rab39_Trichoplax_adhaerens_XP_002114707.1^
64
86
55
98
95
100
98
79
99
78
71
59
100
56
Rab39b
Rab39a
B
Human_RAB39B ---MEAIWLYQFRLIVIGDSTVGKSCLIRRFTEGRFAQV----SDPTVGVDFFSRLVEIE
Mouse_Rab39b ---MEAIWLYQFRLIVIGDSTVGKSCLIRRFTEGRFAQV----SDPTVGVDFFSRLVEIE
Opossum_Rab39b ---MEAIWLYQFRLIVIGDSTVGKSCLIRRFTEGRFPQV----SDPTVGVDFFSRLVEIE
E.Shark_Rab39b MSAMNPEYDYLFKLLLIGDSGVGKSCLLLRFADDTYTES----YISTIGVDFKIRTIELE
Human_RAB39A ---METIWIYQFRLIVIGDSTVGKSCLLHRFTQGRFPGLRSPACDPTVGVDFFSRLLEIE
Mouse_Rab39a ---METIWIYQFRLIVIGDSTVGKSCLLHRFTQGRFPGLHSPACDPTVGVDFFSRLLEIE
Opossum_Rab39a ---MEAIWIYQFRLIVIGDSTVGKSCLLHRFTQGRFPGMLSPACDPTVGVDFFSRLLEIE
E.Shark_Rab39a ---MEAIWIYQFRLIVIGDSTVGKSCLLRRFTDGRFTDV----SDPTVGVDFFARLVEIE
Human_RAB39B PGKRIKLQIWDTAGQERFRSITRAYYRNSVGGLLLFDITNRRSFQNVHEWLEETKVHVQP
Mouse_Rab39b PGKRIKLQIWDTAGQERFRSITRAYYRNSVGGLLLFDITNRRSFQNVHEWLEETKVHVQP
Opossum_Rab39b PGKRIKLQIWDTAGQERFRSITRAYYRNSVGGLLLFDITNRRSFQNVHEWLEETKVHVQP
E.Shark_Rab39b -GKTIKLQIWDTAGQERFRSITRAYYRNSVGGLLLFDITNRRSFQNVHEWLQEAKVHVQP
Human_RAB39A PGKRIKLQLWDTAGQERFRSITRSYYRNSVGGFLVFDITNRRSFEHVKDWLEEAKMYVQP
Mouse_Rab39a PGKRIKLQLWDTAGQERFRSITRSYYRNSVGGFLVFDITNRRSFEHVKDWLEEAKMHVQP
Opossum_Rab39a PGKRIKLQLWDTAGQERFRSITRSYYRNSVGGFLVFDITNRRSFEHVQDWLEEAKMYVQP
E.Shark_Rab39a PGKRIKLQLWDTAGQERFRSITRSYYRNSVGGLLVFDITNRRSFEHVRHWLEEAKMHVQP
Human_RAB39B YQIVFVLVGHKCDLDTQRQVTRHEAEKLAAAYGMKYIETSARDAINVEKAFTDLTRDIYE
Mouse_Rab39b YQIVFVLVGHKCDLDTQRQVTRHEAEKLAAAYGMKYIETSARDAINVEKAFTDLTRDIYE
Opossum_Rab39b YQIVFVLVGHKCDLDTQRQVTRHEAEKVAAGYGMKYIETSARDAINVEKAFTDLTREIYE
E.Shark_Rab39b FQIVFVLVGHKCDLAAQRHVSREEAEKLAAAYHMKYIETSARDSINVEQAFTELTRDIYE
Human_RAB39A FRIVFLLVGHKCDLASQRQVTREEAEKLSADCGMKYIETSAKDATNVEESFTILTRDIYE
Mouse_Rab39a FQIVFLLVGHKCDLASQRQVSREEAERLSTDCGMKYIETSAKDATNVEESFTILTRDIYE
Opossum_Rab39a FRIVFLLVGHKCDLVSQRQVSREEAEKMSAACGMKYIETSAKDATNVEESFTILTRDIYE
E.Shark_Rab39a FQIIFLLVGHKSDLASQRKVSREEAEKLAAVSGMKYIETSAKDATNVEESFTILTREIYG
Human_RAB39B LVKRGEITIQEGWEGVKSGFVPNVVHSSEEVVKSERRCLC
Mouse_Rab39b LVKRGEITIQEGWEGVKSGFVPNVVHSSEEVIKSERRCLC
Opossum_Rab39b LVKRGEITIQEGWEGVKSGFVPNVVHSSEEVVKSDRRCLC
E.Shark_Rab39b LVRRGEITMQEGWEGVKSGFVPNVVHSSEEAVKSGRRCFC
Human_RAB39A LIKKGEICIQDGWEGVKSGFVPNTVHSSEEAVKPRKECFC
Mouse_Rab39a LIKKGEICIQDGWEGVKSGFVPNTVHSSEEAVKPRKECFC
Opossum_Rab39a LIKKGEICIQDGWEGVKSGFVPNIVHSSEEAAKPMKQCIC
E.Shark_Rab39a LLKKGDIGIQEGWEGVKSGFVPNVVHSSEEAVKPGRKCLC
p.Thr168 of RAB39B

Figure S3: RAB39B is conserved across evolution

Molecular phylogenetic analysis was performed by the maximum likelihood method based on the Jones-Taylor-Thornton matrix (Molecular Evolution and Genomic Analysis Version 5.2.2). (A) Following whole genome duplication that occurred early in the vertebrate linage, *Rab39* specified into *Rab39a* and *Rab39b*. Numbers represent the percentage of 1000 bootstraps that reproduced the partition; those with less than 50% replicates have been collapsed. Accession numbers are shown, *determined by TBLATN on genomic sequence, ^partial sequence. (B) Clustal Omega alignment of Rab39a and Rab39b orthologues depicting the conservation of Thr168 and Leu60 in both proteins. Secondary structural motifs for Rab1a (PDB ID: 3TKL) are shown above the alignment where α-helices are represented as cylinders and β-strands as arrows. G1-5 box motifs (defined by the Conserved Domain Database) are shown in bold, and Switch I and Switch II are shaded orange and blue, respectively.

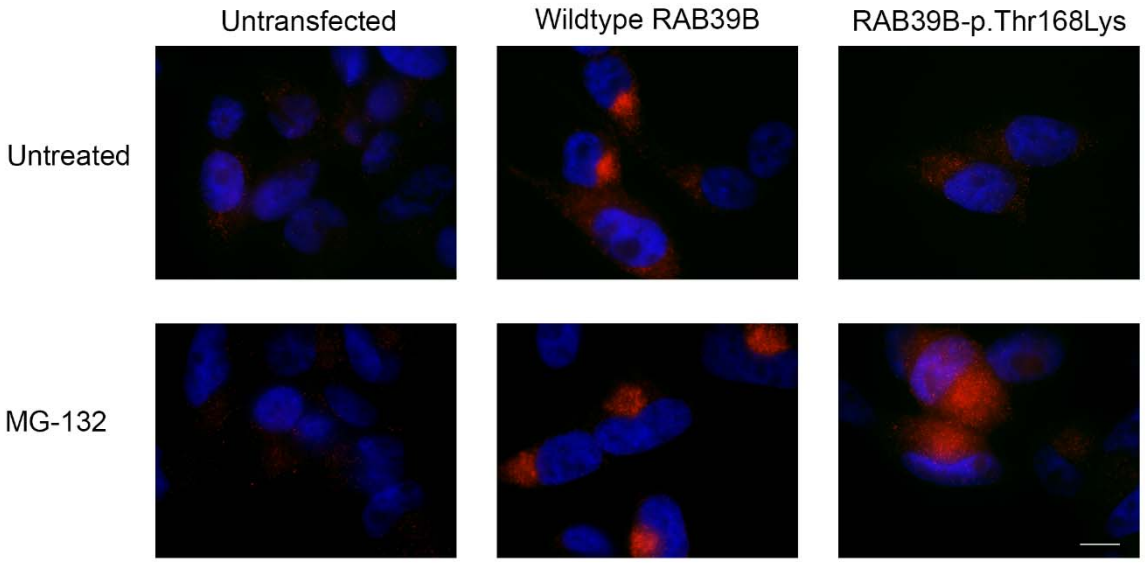

Figure S4: Immunofluorescence analysis suggests that mutant RAB39B-p.Thr168Lys is unstable and degraded by the ubiquitin proteasome system

Immunofluorescence was used to detect endogenous or exogenous RAB39B in BE(2)-M17 neuroblastoma cells, in the absence or presence of 10μM MG-132. Endogenous RAB39B appeared as faint but distinct puncta within the cytoplasm. In the absence of MG-132 wildtype RAB39B recombinant protein was highly expressed and distributed throughout the cytoplasm. In contrast, cells expressing mutant RAB39B-p.Thr168Lys demonstrated a low level of immunoreactivity, equivalent to that observed in the untransfected cells. The steady state level of mutant RAB39B-p.Thr168Lys immunoreactivity increased significantly following MG-132 treatment. Scale bar 10μm.

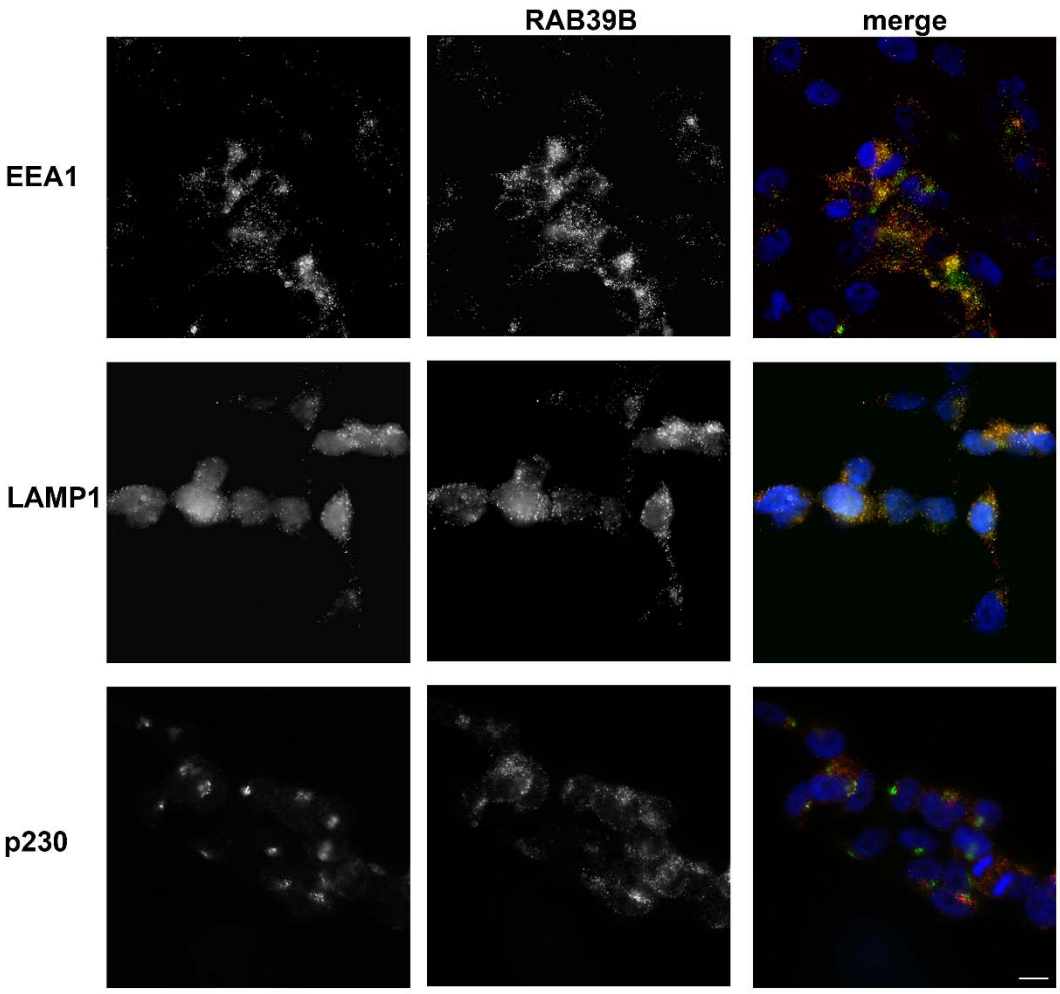

Figure S5: RAB39B co-localizes with markers of the endosomal pathway

The cellular distribution of endogenous RAB39B in BE(2)-M17 neuroblastoma cells was assessed using immunofluorescence co-localization studies. Top panels show co-localization of Early Endosome Antigen 1 (EEA1, green, Santa Cruz Biotechnology Inc, sc-6414, 1:200) with RAB39B (red). The middle panels show co-localization of Lysosomal-associated membrane protein 1 (LAMP1, green, Santa Cruz Biotechnology Inc, sc-80980, 1:200) with RAB39B (red). The bottom panels demonstrate little co-localization of a trans-golgi marker (p230, green, BD Transduction Laboratories, 611280, 1:200) with RAB39B (red). Scale bar 10µm.

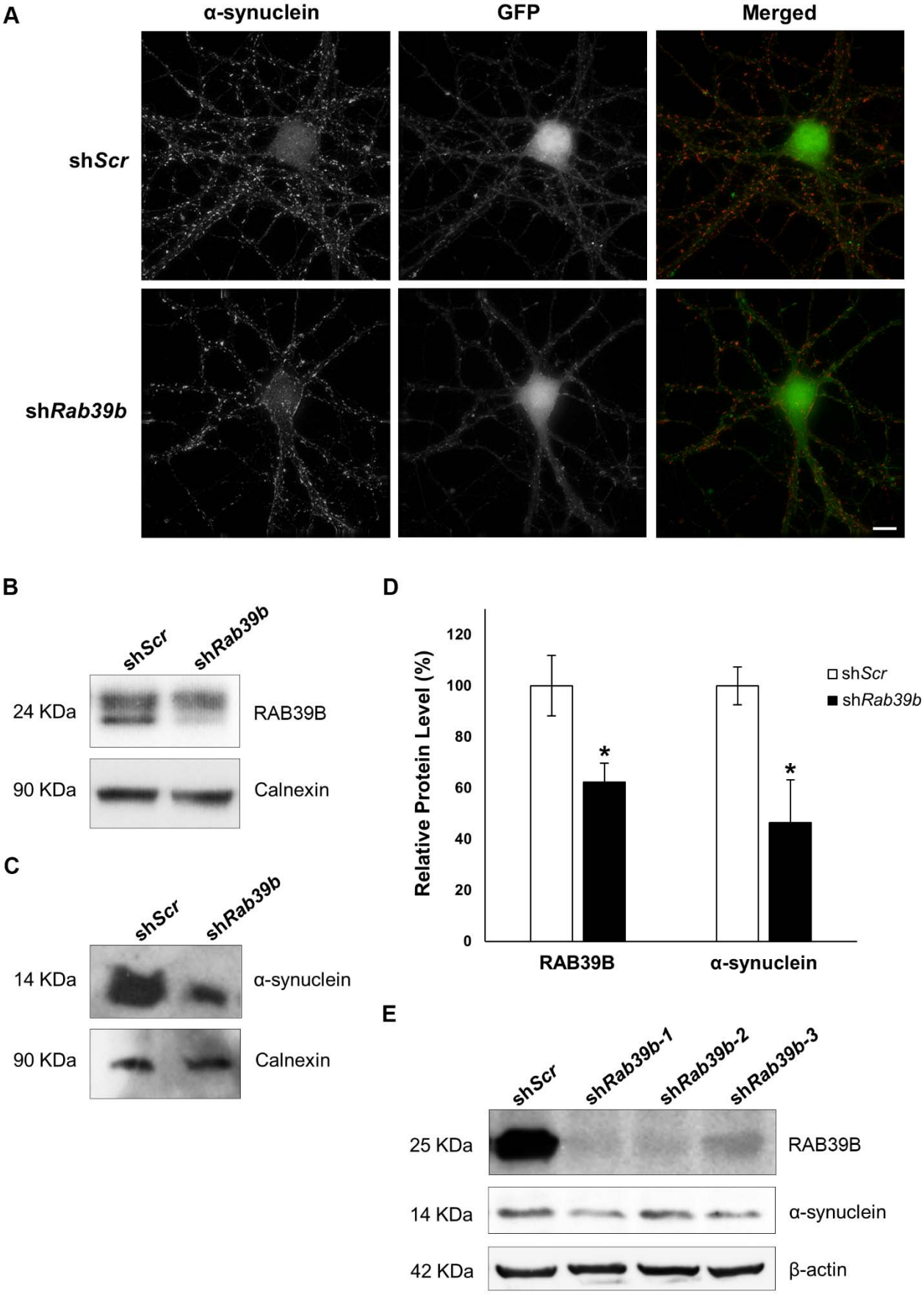
A
α-synuclein
GFP
Merged
shScr
shRab39b
B
shScr
shRab39b
24 KDa
RAB39B
90 KDa
Calnexin
C
shScr
shRab39b
14 KDa
α-synuclein
90 KDa
Calnexin
D
Relative Protein Level (%)
120
100
80
60
40
20
0
shScr
shRab39b
*
*
RAB39B
α-synuclein
E
shScr
shRab39b-1
shRab39b-2
shRab39b-3
25 KDa
RAB39B
14 KDa
α-synuclein
42 KDa
β-actin

Figure S6: Down regulation of *Rab39b* alters α-synuclein homeostasis

Mouse E18 hippocampal neurons were transduced with lentiviral vectors encoding GFP and either scramble (sh*Scr*) or sh*Rab39b* sequences. (A) Robust numbers of α-synuclein immunoreactive puncta were observed in the dendrites of sh*Scr* control neurons compared to sh*Rab39b* transduced neurons. Scale bar 10μm. (B) Immunoblot of transduced neurons with antibodies directed against RAB39B and calnexin. (C) Immunoblot of transduced neurons with antibodies directed against α-synuclein and calnexin. (D) Quantification of (B) and (C) showed a reduction in the steady state levels of RAB39B and α-synuclein in neurons transduced with sh*Rab39b* compared to sh*Scr*. The immunoreactive signals were quantified with a LAS4000 imager and normalized to the loading control calnexin. Protein levels are expressed relative to sh*Scr* transduced neurons adjusted to 100%. The experiments were performed at least three times. * denotes $P \leq 0.05$. (E) Immunoblot of mouse P19 cells transduced with lentiviral vectors encoding either scramble (sh*Scr*) or three independent sh*Rab39b* sequences with antibodies directed against RAB39B, α-synuclein and β-actin. Quantification showed a reduction in the steady state levels of RAB39B (16±4.6%, mean±SEM, $P \leq 0.0005$) and α-synuclein (53±3.8%, mean±SEM, $P \leq 0.005$) in cells transfected with sh*Rab39b* sequences compared to sh*Scr*.

Clinical features	**Australian Kindred**			**Wisconsin Kindred**	**XLMR Families**
Previous description	NA	NA	NA	Ref 1,2	Ref 3,4
Person or Pedigree/s	Person II:3	Person II:2	Person II:1	Wisconsin pedigree	D-23 and MRX72 pedigrees
RAB39B mutation	Deletion	Deletion	Deletion	Point mutation	Nonsense/Splice site
Intellectual disability					
Onset Age (*age at clinical evaluation or retrospective assessment)	<2yr	<2yr	<2yr	<2yr	10-52yr (D-23)/Childhood-46yr (MRX72) *
Pregnancy/birth	Normal	Normal	Normal	Normal	Normal
Early motor milestones	Delayed	Normal	Normal	Delayed	Delayed (±)
Speech initiation	Delayed	Delayed	Delayed	Delayed	Delayed (±)
Early learning difficulties	✓	✓	✓	✓	✓ (±)
Intellectual disability	✓	✓	✓	✓	✓
Able to read and write	×	✓	✓	✓read (±)	✓read (±)
Independent living	×	×	×	✓	NR
Behavioral features					
Obsessional behavior	✓	×	×	NR	NR
Ritualistic behavior	✓	×	×	NR	NR
Hyperactive/disruptive	NR	NR	NR	✓(1/6)	NR
Extrapyramidal symptoms and parkinsonism					
Age at tremor onset	Late childhood	38	44	10-20's	NR
Age at parkinsonism diagnosis	NA	44	45	20's	NR
parkinsonism classification	NA	Akinetic-rigid	Akinetic-rigid	NR	NR
Postural/upper limb tremor	✓	✓	✓	✓(4/6)	NR
Choreoathetosis	×	×	×	✓(1/6)	NR
Shuffling gait	×	✓	✓	✓(5/6)	NR
Bradykinesia	×	✓	✓	✓	NR
Dyskinesia	×	✓	✓	NR	NR
Cogwheel rigidity	×	✓	✓	✓	NR
L-Dopa response	NA	✓	✓[b]	× (3/3)	NA
Hyopkinetic dysarthria	×	✓	✓	✓	NR
Cerebellar function	Normal	Normal	Normal	Normal	NR
Other					
Autism	×	×	×	NR	✓ (3/12)
Seizures	×	×	×	✓ (2/6)	✓ (3/12)
Macrocephaly	✓	✓	✓	✓	✓
Frontal bossing	×	×	×	✓±	NR
Normal eye examination	✓	✓	✓	✓(4/6)	✓
Strabismus	×	×	×	✓(1/6)	NR
Iris Coloboma	×	×	×	✓ (1/6)	NR
Hydrops	×	×	×	✓(1/6)	NR
Dysmorphism	×	×	×	NR	×
High arched palate	×	×	×	✓(5/6)	NR
Dementia	×	×	✓	NR	NR
Skin depigmented papules	×	×	×	✓4/6	NR
Additional Tests					
MRI	NA	Normal	Abnormal[c]	NA	Normal
Fragile X	Normal	Normal	Normal	Normal	Normal (±)
Karyotype	Normal	Normal	Normal	Normal	NR
CT scan	NA	NA	NA	Megalencephaly	Normal
Copper testing	Normal	Normal	Normal	Normal	NR
Blood count and chemistry	Normal	Normal	Normal	Normal	NR
Urine metabolic testing	Normal[a]	Normal	Normal	Normal	NR
EEG	×	×	×	Abnormal (2/6)	NR
Hearing	Normal	Normal	Normal	Normal	NR

Table S1: Clinical description of the males with mutations in *RAB39B*.

The clinical features of the Australian and Wisconsin kindreds are described in detail. Note that the clinical features of the Wisconsin pedigree are based on the 6 male individuals described previously[5,6]. Two XLMR pedigrees, D-23 and MRX72, presenting with mental retardation and macrocephaly were described previously[14,16].

✓ or × indicates the feature is present or absent in the described individual/pedigree, respectively. In cases where not all of the individuals/pedigrees displayed the trait, the number of affected individuals/pedigrees is defined in brackets. Alternatively, ± indicates the phenotype is present in several individuals or pedigrees but specific number was not defined.

[a] Urine test had borderline MPS; [b] side effects to L-Dopa; [c] T2 weighted MRI showed slight bilateral reduction in signal intensity in the substantia nigra and globus pallidus, indicative of iron/calcium deposition. Blood count and chemistry includes: liver function, calcium, uric acid, serum ceruplasmin/copper/lead/zinc/lipoprotein and parathyroid hormone. NR is not reported. CSF is cerebral spinal fluid; NA is not applicable.

Linkage region 1	Marker	HGSV reference
Beginning	rs17051658	NC_000023.11:g.3624034
End	rs16979497	NC_000023.11:g.14291092
Linkage region 2		
Beginning	rs1174432	NC_000023.11:g.145644895
End	Telomere	NA

GRCh38 assembly, annotation release 106

Table S2: X-chromosome linkage regions identified in the Australian kindred.

Genomic DNA from the mother and 5 offspring of the Australian kindred were genotyped using high density Illumina 610-quad beadchip SNP arrays at the Australian Genome Research Facility. Genotypes were called using the GenCall algorithm implemented in Illumina's BeadStudio package and the likelihood of inbreeding was established using FEStim. A subset of ~10,000 SNPs spaced at least 0.15 cM apart were selected for linkage analysis. Parametric linkage analysis using a rare recessive disease model and haplotype reconstruction were performed using MERLIN. Linkage regions were interrogated for CNV (Copy Number Variation) using Genome Studio software and CNV results were filtered with reference to the Database of Genomic Variants (DGV).

Gene	Position (hg19)	Mutation	PolyPhen	SIFT	Sample	CADD score
RAB39B*	X:154490014	Deletion (>19373bp)	NA	NA	II:2	NA
MBNL3	X:131573578	C>G p.Arg21Thr	probably damaging	damaging	II:2	23.90
MAGEA4*	X:151092942	G>A p.Arg269His	benign	NA	II:2	7.36
RAB39B*	X:154490227	G>T p.Thr168Lys	probably damaging	damaging	IV:12	22.60
FANCB	X:14882764	A>G p.Met290Thr	possibly damaging	tolerated	IV:12	10.43
CETN2*	X:151997804	C>T p.Lys60Lys	NA	NA	IV:12	8.94
HEPH	X:65382607	A>G p.Asn13Ser	NA	NA	IV:12	6.00
RBMXL3	X:114426769	A>G p.Asn922Ser	benign	NA	IV:12	5.20
NLGN4X	X:6069437	T>C p.Asn24Ser	benign	tolerated	IV:12	0.01

Table S3: List of novel variants identified by X-exome sequencing in the Australian and Wisconsin kindreds.

X-Exome sequencing and analysis of gDNA by droplet-based multiplex PCR was performed essentially as previously described[5]. Variants identified in individuals II:2 (Australian kindred) and IV:12 (Wisconsin kindred) were filtered against dbSNP138 (http://www.ncbi.nlm.nih.gov/snp), 1000Genomes (release20110521), and NHLBI Exome Sequencing Project (ESP6500). Variants were subsequently ranked by potential functional impact using the CADD score[6]. NA = not applicable. *-variants within the haplotype/linkage region. Variants identified in *RAB39B* have been submitted to the NCBI ClinVar database.

Supplemental References

1. Laxova, R., Brown, E.S., Hogan, K., Hecox, K., and Opitz, J.M. (1985). An X-linked recessive basal ganglia disorder with mental retardation. American journal of medical genetics 21, 681-689.
2. Gregg, R.G., Metzenberg, A.B., Hogan, K., Sekhon, G., and Laxova, R. (1991). Waisman syndrome, a human X-linked recessive basal ganglia disorder with mental retardation: localization to Xq27.3-qter. Genomics 9, 701-706.
3. Giannandrea, M., Bianchi, V., Mignogna, M.L., Sirri, A., Carrabino, S., D'Elia, E., Vecellio, M., Russo, S., Cogliati, F., Larizza, L., et al. (2010). Mutations in the small GTPase gene RAB39B are responsible for X-linked mental retardation associated with autism, epilepsy, and macrocephaly. American journal of human genetics 86, 185-195.
4. Russo, S., Cogliati, F., Cavalleri, F., Cassitto, M.G., Giglioli, R., Toniolo, D., Casari, G., and Larizza, L. (2000). Mapping to distal Xq28 of nonspecific X-linked mental retardation MRX72: linkage analysis and clinical findings in a three-generation Sardinian family. American journal of medical genetics 94, 376-382.
5. Hu, H., Wrogemann, K., Kalscheuer, V., Tzschach, A., Richard, H., Haas, S.A., Menzel, C., Bienek, M., Froyen, G., Raynaud, M., et al. (2009). Mutation screening in 86 known X-linked mental retardation genes by droplet-based multiplex PCR and massive parallel sequencing. The HUGO journal 3, 41-49.
6. Kircher, M., Witten, D.M., Jain, P., O'Roak, B.J., Cooper, G.M., and Shendure, J. (2014). A general framework for estimating the relative pathogenicity of human genetic variants. Nature genetics 46, 310-315.